Clim. Past Discuss., 7, 2193–2215, 2011
www.clim-past-discuss.net/7/2193/2011/
doi:10.5194/cpd-7-2193-2011

Climate of the Past Discussions

High-latitude obliquity forcing drives the agulhas leakage

T. Caley[1], J.-H. Kim[2], B. Malaizé[1], J. Giraudeau[1], T. Laepple[3], N. Caillon[4], K. Charlier[1], H. Rebaubier[4], L. Rossignol[1], I. S. Castañeda[2], S. Schouten[2], and J. S. S. Damsté[2]

[1]Environnements et paléoenvironnements océaniques, UMR5805, CNRS – Université de Bordeaux 1, EPOC, France
[2]NIOZ Royal Netherlands Institute for Sea Research, Department of Marine Organic Biogeochemistry, 1790 AB Den Burg, The Netherlands
[3]Alfred Wegener Institut (AWI), Germany
[4]Laboratoire des Sciences du Climat et de l'Environnement, LSCE, Gif-sur-Yvette, France

Received: 27 June 2011 – Accepted: 28 June 2011 – Published: 30 June 2011

Correspondence to: T. Caley (t.caley@epoc.u-bordeaux1.fr)

Published by Copernicus Publications on behalf of the European Geosciences Union.

Abstract

The Agulhas Current (AC) transport of heat and salt from the Indian Ocean into the South Atlantic around South Africa (Agulhas leakage), has a profound role in the decadal variability of the Atlantic meridional overturning circulation (AMOC), which influences global climate. On glacial-interglacial timescales, paleostudies postulate that Agulhas leakage plays a decisive role for AMOC resumption during terminations (glacial-interglacial transitions). However, efforts to elucidate forcing mechanisms connecting Agulhas leakage with glacial-interglacial AMOC variability have been hampered due to a lack of climate records extracted from the area where the AC originates. Here we present 800-kyr sea surface temperature (SST) and salinity (SSS) records from the "precursor" region of the AC. These records contain strong obliquity-driven 41-kyr cycles, nearly in phase with changes in annual mean insolation and air temperature at high southern latitudes. In contrast, precession-driven cycles were negligible in our SST records, which is surprising given the low-latitude location of the Agulhas leakage. Together, this suggests that long-term Agulhas leakage dynamics are associated with a high latitude rather than a tropical climate forcing mechanism, probably by varying the position of the Southern Hemisphere subtropical convergence (STC) and its associated westerlies. We argue that during terminations stronger Agulhas leakage was triggered by increased obliquity exerting a positive feedback on the global climate system through modulating long-term AMOC variations.

1 Introduction

The AC is a key component of the global ocean "conveyor" circulation controlling the inter-ocean exchange of heat and salt (Agulhas leakage) (Weijer et al., 2002; Gordon, 2003; Lutjeharms, 2006; Beal et al., 2011). Modelling studies show that mesoscale eddies, so-called "Agulhas rings", transport and release warm and salty Indian Ocean waters into the South Atlantic, altering the buoyancy of Atlantic thermocline waters and influencing North Atlantic deep-water formation (Weijer et al., 2002) and, thus AMOC variability (Biastoch et al., 2008). Accurate knowledge of the mechanisms governing the dynamics and strength of the Agulhas leakage under different climatic conditions is therefore essential for properly constraining the long-term AMOC response to the Agulhas leakage in climate models (Gordon, 2003), for better understanding the evolution of global climate, and for credible long-term climate predictions. However, long-term SSS records are scarce in the Agulhas system and, to date, most of SST records were reconstructed either in the Agulhas ring region (Peeters et al., 2004; Martinez Mendez et al., 2010) or outside of the AC trajectory (Bard and Rickaby, 2009).

Here we present 800-kyr records of SST and changes in the $\delta^{18}O$ of surface water ($\Delta\delta^{18}O_{sw}$, a proxy of regional SSS) from a sediment core located beneath the present "precursor" region of the AC (MD96-2048, 26°10′482 S, 34°01′148 E, 660 m water depth, Fig. 1). We examine the effects of SST and SSS variations on changes in AC strength and Agulhas leakage.

2 Material and methods

Core MD96-2048 (37.59 m) was collected during the 104 MOZAPHARE oceanographic cruise of the R/V *Marion Dufresne*. This study was conducted on the top 12 m of core MD96-2048 which accumulated at an average rate of 2 cm kyr^{-1}.

2.1 Isotope analysis

The core was sampled every 2-5 cm for isotope analysis ($\delta^{18}O$). For each analysis, 4 to 6 specimens of planktonic *G. ruber s. s.* and benthic *P. wuellerstorfi* foraminifera were picked within the 250–315 µm size fraction. Analyses were carried out by a coupled system Multiprep-Optima of the mark Micromass at EPOC. The automated system of preparation (Multiprep) transforms carbonate samples (50 to 100 µg of calcium carbonate) to CO_2 gas evolved by treatment with ortho-phosphoric acid at a constant

CPD
7, 2193–2215, 2011

temperature of 75 °C. The CO_2 gas samples were then analysed by the isotope mass spectrometer (Optima) in comparison with a calibrated reference gas to determine the isotopic ratio $^{18}O/^{16}O$ of the sample. For all stable oxygen isotope measurements a working standard (Burgbrohl CO_2 gas) was used, which was calibrated against Vienna Pee Dee Belemnite (VPDB) by using the NBS 19 standard. Consequently, all $\delta^{18}O$ data given here are relative to the VPDB standard. Analytical standard deviation is about 0.05 % ($\pm 1\sigma$).

2.2 Mg/Ca analysis

Core MD96-2048 was sampled every 2–5 cm for Mg/Ca analysis. 25 specimens of *G. ruber s. s.* were picked within the 250–315 µm size fraction for trace element analyses. Shells were cleaned to eliminate contamination from clays and organic matter based on the procedure of Barker et al. (2003). A Varian Vista Pro Inductively Coupled Plasma Optical Emission Spectrometer (ICP-OES) was used for magnesium and calcium analyses following the procedure established at LSCE (De Villiers et al., 2002). Reproducibility obtained from *G. ruber s. s.* samples was better than 4 % ($\pm 1\sigma$, pooled RSD). For Mg/Ca ratios determined with a standard solution of Mg/Ca (5.23 mmol/mol), analytical precision was 0.5 % ($\pm 1\sigma$, RSD). All the analyses were performed at LSCE, which participated in an inter-calibration exercise (Greaves et al., 2008). Measured Mg/Ca ratios were converted into temperature values applying the equation established by Anand et al. (2003) yielding a precision of 1.2 °C.

2.3 Alkenone and GDGTs analysis

Core MD96-2048 was sampled every 5–10 cm for alkenone and glycerol dialkyl glycerol tetraether (GDGT) analysis. Freeze-dried and grounded sediments were extracted with a Dionex Accelerated Solvent Extractor using a 9:1 (v/v) mixture of dichloromethane and methanol at NIOZ. After extraction, a known amount (1 µg) of C_{46} GDGT internal standard was added to the total extracts. The extracts were separated by Al_2O_3

CPD
7, 2193–2215, 2011

column chromatography using hexane/DCM (9:1, v/v), hexane/DCM (1:1, v/v), and DCM/MeOH (1:1, v/v) as subsequent eluents. A known amount of an internal standard, a deuterated ante-iso C_{22} alkane, was added to the alkenone fraction (hexane:DCM, 1:1 v/v) for quantification. The alkenone fraction (hexane/DCM, 1:1, v/v) was analyzed by a gas chromatography (Agilent 6890). The $U_{37}^{K'}$ was calculated as defined by Prahl and Wakeham (Prahl and Wakeham, 1987). The $U_{37}^{K'}$ values were converted into temperature values applying the culture calibration by Prahl et al. (1988) yielding a precision of 1.2 °C, which has also been validated by core-top calibration (Müller et al., 1998). The analytical precision of the method is about 0.3 °C.

The polar fraction (DCM/MeOH, 1:1, v/v), containing GDGTs, was analyzed using a high-performance liquid chromatography/atmospheric pressure chemical ionization-mass spectrometry. GDGTs were detected by single ion monitoring of their $(M + H)^+$ ions and quantification of the GDGT compounds was achieved by integrating the peak areas and using the internal standard (C_{46} GDGT). The TEX_{86}^{H} ratio was calculated as defined by Kim et al. (2010) and the TEX_{86}^{H} values were converted into temperature using the calibration of Kim et al. (2010) yielding a precision of 2.5 °C. The analytical precision of the method is about 0.2 °C.

2.4 δ^{18}Osw reconstruction (proxy of SSS)

For the sea surface salinity (SSS) reconstruction, we followed the method developed by (Duplessy et al., 1991) which leans on the double influence of surface temperature and the δ^{18}Osw isotopic composition of seawater on the isotopic values of the planktonic foraminifera (*G. ruber* s. s.). The isotopic temperature signals (Mg/Ca-SST) are subtracted from the planktonic δ^{18}O record (*G. ruber s. s.*). The residual signal can be interpreted in terms of past δ^{18}Osw variations (linked to SSS variations). An additional correction, linked to variation effect of continental ice (due to glacial-interglacial changes) has been applied to get the final $\Delta\delta^{18}$Osw signal (Bintanja et al., 2005). Uncertainties of $\Delta\delta^{18}$Osw estimates were obtained with an error propagation calculation

CPD
7, 2193–2215, 2011

(errors of Mg/Ca-SST (1.2 °C) and planktonic δ^{18}O measurements (0.05 ‰)) using the formula of Press et al. (1990) and the obtained uncertainty of $\Delta\delta^{18}$Osw estimates was 0.26 ‰ ($\pm 1\sigma$).

2.5 Spectral estimates

For spectral estimates, the proxy records are linearly interpolated to a uniform spacing of 0.5 kyr. The power spectral density, coherence and phase are estimated using a smoothed periodogram (Bloomfield, 1976). Before the analysis, a split cosine bell taper is applied to 10 % of the data at the beginning and end of the series. To estimate the significance of the power spectral density, the spectrum background is estimated by fitting an analytical red noise spectrum to the median-smoothed spectrum estimate (Mann and Lees, 1996). The confidence intervals are calculated under the assumption that the spectral estimates are chi-square distributed (Percival and Walden, 1993). The degrees of freedom of the spectral estimate are 8 for the power spectral density calculation and 19 for the phase and coherency calculation. Our statistical procedure of estimating the significance of the sample coherence and the confidence intervals of the phase estimate largely follows Huybers and Denton (Huybers and Denton, 2008). To estimate the significance of the coherence, we use a Monte Carlo procedure to estimate the 95 % significance level. Therefore, one of the two time-series is replaced by a red-noise process using the estimated lag-1 auto-covariance. The coherence is estimated 10 000 times on the surrogate time series. The uncertainty in the phase estimated is also estimated using a Monte Carlo procedure. Using white noise realizations, a signal according to the degree of coherence estimated from the data is generated. Here, the bias-corrected coherence estimate is used (Amos and Koopmans, 1963). The algorithm is repeated 10 000 times to estimate the 95 % confidence intervals for the phase estimate.

3 Results

Characteristic glacial-interglacial changes in the down-core record of stable oxygen isotopic composition of the benthic foraminifer *Planulina wuellerstorfi* ($\delta^{18}O_{benthic}$, Fig. 2a) served as control points for the age model tuned to the LR04 stack (Lisiecki and Raymo, 2005) (Fig. S1), and allowed for the identification of eight terminations. The age model of Lisiecki and Raymo, (2005), constrains ages by aligning variations in the benthic foraminifera $\delta^{18}O$ record with variations in the orbital parameters. It has been criticised that this approach precludes an objective evaluation of the orbital influence on glacial timing (Huybers, 2007). We therefore established an additional age model not relying upon orbital assumptions, by tuning the benthic $\delta^{18}O$ record to the depth-derived age model (Huybers, 2007) (Fig. S1). In general, the H07-based age model strongly resembles the LR04-based one. However, both age models deviate from each other for the time interval between MIS 7 and MIS 9.

We applied three independent inorganic and organic paleothermometers to reconstruct AC SST changes: Mg/Ca ratios of the surface-dwelling planktonic foraminifer *Globigerinoides ruber sensu stricto*, alkenone unsaturation index ($U^{K'}_{37}$) from haptophyte algae, and tetraether index (TEX^{H}_{86}) of Group I Crenarchaeota. Measuring three independent proxies is important to crosscheck temperature variations. All three records are strongly related between each other ($R > 0.5, p < 0.01$) and exhibit typical glacial-interglacial patterns (Fig. S2). As each proxy has some uncertainty related to the calibration, non-temperature influences and lateral advection, the three records were averaged into a single SST stack (Fig. 2b). It is reasonable to assume that the uncertainties are independent between the proxy types. Therefore, the stack is a more accurate temperature reconstruction than the usual interpretation of single temperature proxy records. It also facilitates visual comparisons with other records and strengthens the common down-core patterns. Before stacking, $U^{K'}_{37}$ and TEX^{H}_{86} signals were linearly interpolated to the same time resolution as the Mg/Ca signal, which is the SST dataset with the highest time resolution. To examine whether the SST stack is representative

CPD
7, 2193–2215, 2011

of coherent down-core temporal variation, we applied Empirical Orthogonal Function (EOF) analysis (Von Storch and Zwiers., 1999) on the three SST records (Fig. S2). An almost identical temporal variation of the first Principal Component (PC1, 74 % variance) and the SST stack ($R > 0.99$) confirms that this record represents the common temporal variation of the three individual SST records. Additionally, we constructed past $\Delta\delta^{18}O_{sw}$ (Fig. 2c), by combining the Mg/Ca SST estimates with the $\delta^{18}O$ values of *G. ruber* and removing the influence of continental ice volume on global $\delta^{18}O_{sw}$.

4 Discussion

4.1 Orbital forcing for agulhas leakage records

Our SST stack and $\Delta\delta^{18}O_{sw}$ records show glacial-interglacial patterns (Fig. 2b–c). Spectral analyses revealed a strong signal in both 100-kyr (glacial-interglacial) and 41-kyr (obliquity) periodicities (Fig. 2d, 3a–b). The origin of the 100-kyr cycle could be linked to eccentricity forcing, to internally-driven climate feedbacks imparting some eccentricity influence (Lisiecki, 2010), or, alternatively, 100-kyr cycles can result from quantized bundles of 41-kyr obliquity cycles (Huybers and Wunsch, 2005). However, the 23-kyr and 19-kyr (precession) signals, which are modulated by eccentricity, are weak in our records (Fig. 3), suggesting that eccentricity forcing plays no significant role at our site. Interestingly, over the last 800 kyr, obliquity signals of SST stack and $\Delta\delta^{18}O_{sw}$ records are nearly in phase with changes in high-latitude annual mean insolation rather than with any local insolation index at 26 °S (Berger and Loutre, 1991) (Fig. 2e) and with the obliquity components of the Antarctic temperatures (Jouzel et al., 2007) (Fig. 2f). Regardless of whether the statistical analysis is performed using an alternative age model (Fig. S4), or with the individual SST records (Fig. S5), the important finding remains that all records vary in phase with changes in high-latitude obliquity. This indicates that a strong influence of local insolation on our records can be excluded; a linear response to local insolation would be out of phase in the obliquity

CPD
7, 2193–2215, 2011

band with the Agulhas records and local seasonal responses, e.g. caused by local nonlinearities (Leapple and Lohmann, 2009), would contain a strong precession component contrary to our observation in the Agulhas records. An important role of the latitudinal insolation gradient (LIG) can also be excluded as it contains both obliquity and precession frequencies as a result of seasonal differences in orbital forcing (Davis and Brewer, 2009). In addition, the LIG has been suggested as the origin of obliquity periodicities evident in the deuterium excess record from the Vostok ice core in Antarctica (Vimeux et al., 1999). However, the deuterium excess record is out of phase in the obliquity band with the Agulhas records as with obliquity components of the Antarctic temperatures (Vimeux et al., 1999).

Changes in high latitude insolation driven by obliquity variations may have controlled the position of the STC along with the shift of the Southern Hemisphere westerlies (Bard and Rickaby, 2009; Biastoch et al., 2009), changes in heat export from the tropics (Jouzel et al., 2007), and sea ice coverage (Knorr and Lohmann, 2003). Poleward shifts of the STC modify recirculation in the Indian subtropical gyre (Bard and Rickaby, 2009), which intensifies heat and salt transfer from the Indian Ocean to the South Atlantic, thus increasing SSTs and SSSs of the AC. Recent observations (Alory et al., 2007) and modelling results (Biastoch et al., 2009) have shown warming/salinification tendencies of the southwest Indian Ocean in relation to a poleward migration of the STC. Interestingly, Antarctic temperature records (Jouzel et al., 2007) also exhibit strong obliquity components (Fig. 2f). Consequently, the in-phase relationship of the obliquity components of the Antarctic temperatures (Jouzel et al., 2009) and the SSTs and SSSs of the AC (Table 1) suggests that variability in AC is coupled to high latitude Southern Hemisphere climate forcing. It should also be noted that the Agulhas leakage fauna (ALF) record, a foraminiferal proxy of Agulhas leakage from the Cape basin (Peeters et al., 2004) and our $\Delta\delta^{18}O_{sw}$ record do show, in addition to obliquity signals, weak signals in the precession band that is absent in our SST records (Fig. S6). Peeters and co-workers proposed a possible link of the Agulhas leakage with low-latitude monsoon forcing to explain the presence of precession signals. However, in contrast to the ALF record, the monsoon records are not in phase with the Northern Hemisphere summer insolation intensity (Clemens et al., 2010; Caley et al., 2011). This suggests that the increased strength of the Indo-Asian monsoon cannot fully explain the timing of the precession signal recorded in the ALF record. Interestingly, the STC record also contains a very weak precession signal (Peeters et al., 2004). This suggests that the precession signal in the Agulhas system might be linked to a high-latitude climate forcing via Southern Hemisphere frontal changes rather than by low latitude climate forcing originated from the Indian Ocean.

4.2 Subtropical convergence migration, agulhas current strength and transfer relationship

Recently, it has been suggested that northward migrations of the STC modulated the severity of each glacial period (particularly during MIS10 and 12 at site MD96-2077) (Bard and Rickaby, 2009). The hypothesis that a northward-migrating STC would block the AC and thus affect water transport from the Indian Ocean to the South Atlantic is still under debate (Rau et al., 2002; Bard and Rickaby, 2009; Zahn, 2009). For the particular and exceptional MIS 12 (extreme northward position of the STC) (Bard and Rickaby, 2009), all records at site MD96-2048 show an early increase in SST whereas the coldest SSTs are observed further to the south at site MD96-2077 (Figs. 1, 2). This suggests that the build-up of heat from the return flow of the AC is linked to the latitudinal contraction of subtropical gyres (Sijp and England, 2008). A comparison of our $U_{37}^{K'}$ SST record with that of MD96-2077 also reveals stronger deviations during the glacial periods, especially MIS 10 and 12 (Fig. 4a–b). Increased glacial SSTs were recorded at site MD96-2048 when the STC reached its northern most position, which may be related to a build-up of heat from the return flow that could not escape to the Atlantic as for MIS 12. Alternatively, lateral fluxes and thus the AC were stronger when Agulhas leakage was weaker (Supplement), which contradicts the existing hypothesis that reduced glacial Agulhas leakage was caused by a weakened AC (Franzese et al., 2009). Although our hypothesis awaits future confirmation, it is in good agreement with some modelling results showing that when the AC is weak, the Indian-Atlantic inter-ocean exchange is larger with westward movement of the Agulhas retroflection (De Ruijter, 1982; Van Sebille et al., 2009).

4.3 Impact of heat and salt agulhas leakage

Our results show that changes in SST and SSS led variations in global ice volume (i.e. benthic δ^{18}O value) on obliquity time-scales (Fig. 3c–d). The time-lags of benthic δ^{18}O are 2.2 kyr (±1.9 kyr, 95 % confidence interval) for SST and 1.7 kyr (±6.1 kyr, 95 % confidence interval) for $\Delta\delta^{18}O_{sw}$ in the obliquity band (Table 1). The ALF variations also led benthic δ^{18}O changes in the Cape basin (Peeters et al., 2004). This suggests that the enhanced leakage of warmer and saltier Indian Ocean waters into the South Atlantic during the terminations allowed for the development of a South-North density gradient in the Atlantic before the global ice volume change, reinforcing the AMOC (Weijer et al., 2002; Biastoch et al., 2008). Recently, Lisiecki et al. (2008) showed that maxima in high northern latitude summer insolation (that is, Milankovitch forcing) are associated with greater mid-depth Atlantic overturning in the obliquity band but with less overturning in the precession band. This is in contrast to the SPECMAP hypothesis that circulation response has the same phase relative to ice volume in all three orbital bands and suggests that the AMOC is more strongly influenced by other factors than ice volume changes and summer insolation at high northern latitudes (Lisiecki et al., 2008). Interestingly, it has also been shown that stronger AMOC during MIS 11 inhibited significant ice-sheet build-up and prolonged the interglacial period at a time of high orbital obliquity (Dickson et al., 2009, 2010). Our results from the Agulhas system provide an important metric for the AMOC response to orbital-obliquity forcing that contributed to global climate changes as a positive feedback.

Obliquity–driven glacial terminations during the late Pleistocene have previously been hypothesized (Huybers and Wunsch, 2005) and is supported by a speleothem record from the Northeast Atlantic region (Drysdale et al., 2009), showing the influence of obliquity and AMOC variations on Termination 2. However, feedback mechanisms that amplified the initial obliquity forcing have not been elucidated yet. AMOC responses to orbital forcing are also highly model-dependent, showing contradictory results (Yoshimori et al., 2001; Khodri et al., 2003). Our finding of obliquity-driven Agulhas leakages sheds light on a new feedback mechanism for long-term AMOC responses to the inter-ocean heat and salt exchange. We suggest that this obliquity signal is transmitted from the Southern Hemisphere to the Northern Hemisphere via AMOC changes. This could explain why AMOC variability is not solely dependent on ice volume and summer insolation at high northern latitudes (Lisiecki et al., 2008).

5 Conclusion

Sea surface temperature and salinity records from the "precursor" region of the Agulhas current contain strong obliquity-driven 41-kyr cycles over the last 800 kyr. This suggests that long-term Agulhas leakage dynamics are associated with high latitude rather than a tropical climate forcing mechanism by varying the position of the Southern Hemisphere subtropical convergence and its associated westerlies.

To trigger ice age terminations, important feedbacks need to be added to the direct effect of insolation changes on ice sheets. We argue that the important transfer of heat and salt via the AC, which affected the resumption of the AMOC and the initiation of interglacial conditions (Weijer et al., 2002; Knorr and Lohmann, 2003; Biastock et al., 2008), is one of the main feedbacks. Intermediate complexity climate models emphasize the important role of Agulhas leakage for AMOC changes (Marsh et al., 2007), while fully coupled ocean-atmosphere models do not resolve the Agulhas leakage (Lohmann, 2003; Beal et al., 2011). Therefore, obliquity-induced variability of the Agulhas leakage merits greater attention in global ocean and climate models used for predicting the future climate scenarios.

Supplementary material related to this article is available online at: http://www.clim-past-discuss.net/7/2193/2011/cpd-7-2193-2011-supplement.pdf.

Acknowledgements. The technical staffs at EPOC, LSCE and NIOZ are thanked for their contributions to sample preparation and measurements. All the members of team PALEO at EPOC are acknowledged for their help and stimulating discussions and E. Bard for commenting on an early draft of the manuscript. Core MD96-2048 was collected during the MOZAPHAR cruise of the RV Marion Dufresne, supported by the French agencies Ministère de l'Education Nationale de la Recherche et de la Technologie, Centre National de la Recherche Scientifique (CNRS), and Institut Paul Emile Victor (IPEV). Financial contribution from the CNRS INSU LEFE-EVE program "MOMIES" is acknowledged.

Institut national des sciences de l'Univers

The publication of this article is financed by CNRS-INSU.

References

Alory, G., Wijffels, S., and Meyers, G.: Observed temperature trends in the Indian Ocean over 1960–1999 and associated mechanisms, Geophys. Res. Lett., 34, L02606, doi:10.1029/2006GL028044, 2007.

Amos, D. and Koopmans, L.: Tables of the distribution of the coefficient of coherence for stationary bivariate Gaussian processes, SCR-483, Sandia Corp, 1963.

Anand, P., Elderfield, H., and Conte, M. H.: Calibration of Mg/Ca thermometry in planktonic foraminifera from a sediment trap time series, Paleoceanography, 18, 1050, doi:10.1029/2002PA000846, 2003.

Bard, E. and Rickaby, E. M.: Migration of the subtropical front as a modulator of glacial climate, Nature, 460, 380–383, 2009.
Barker, S., Greaves, M., and Elderfield, H.: A study of cleaning procedures used for foraminiferal Mg/Ca paleothermometry, Geochem. Geophy. Geosys., 4, 8407, doi:10.1029/2003GC000559, 2003.
Beal, L. M., De Ruijter, W. P. M., Biastoch, A., Zahn, R., SCOR/WCRP/IAPSO Working Group 136.: On the role of the Agulhas system in ocean circulation and climate, Nature, 472, 429–436, 2011.
Berger, A. and Loutre, M.: Insolation values for the climate of the last 10 million years,. Quat. Sci. Rev., 10, 297–317, 1991.
Biastoch, A., Boning, C. W., and Lutjeharms, J. R. E.: Agulhas leakage dynamics affects decadal variability in Atlantic overturning circulation, Nature, 456, 489–492, 2008.
Biastoch, A., Boning, C. W., Schwarzkopf, F. U., and Lutjeharms, J. R. E.: Increase in Agulhas leakage due to poleward shift of Southern Hemisphere westerlies, Nature, 462, 495–498, 2009.
Bintanja, R., Van de Wal, R., and Oerlemans, J.: Modelled atmospheric temperatures and global sea levels over the past million years, Nature, 437, 125–128, 2005.
Bloomfield, P.: Fourier analysis of time series: An introduction, Wiley, New York, 1976.
Caley, T., Malaizé, B., Zaragosi, S., Rossignol, L., Bourget, J., Eynaud, F., Martinez, P., Giraudeau, J., Charlier, K., and Ellouz-Zimmermann, N.: New Arabian Sea records help decipher orbital timing of Indo-Asian monsoon, Earth Planet. Sci. Lett., in press, 2011.
Clemens, S. C., Prell, W. L., and Sun, Y.: Orbital-scale timing and mechanisms driving Late Pleistocene Indo-Asian summer monsoons: Reinterpreting cave speleothem δ18O, Paleoceanography, 25, PA4207, doi:10.1029/2010PA001926, 2010.
Davis, B. A. S. and Brewer, S.: Orbital forcing and role of the latitudinal insolation/temperature gradient, Clim. Dyn., 32, 143–145, 2009.
De Ruijter, W.: Asymptotic analysis of the Agulhas and Brazil Current systems, J. Phys. Oceanogr., 12, 361–373, 1982.
De Villiers, S., Greaves, M., and Elderfield, H.: An intensity ratio calibration method for the accurate detremination of Mg/Ca and Sr/Ca of marine carbonates by ICP-AES, Geochem. Geophy. Geosys., 3, 1001, doi:10.1029/2001GC000169, 2002.
Dickson, A. J., Beer, C. J., Dempsey, C., Maslin, M. A., Bendle, J. A., McClymont, E. L., and Pancost, R. D.: Oceanic forcing of the Marine Isotope Stage 11 interglacial, Nature Geosci.,

2, 428–433, 2009.
Dickson, A. J., Leng, M. J., Maslin, M. A., Sloane, H. J., Green, J., Bendle, J. A., McClymont, E. L., and Pancost, R. D.: Atlantic overturning circulation and Agulhas leakage influences on southeast Atlantic upper ocean hydrography during marine isotope stage 11, Paleoceanography, 25, PA3208, doi:10.1029/2009PA001830, 2010.
Drysdale, R. N., Hellstrom, J. C., Zanchetta, G., Fallick, A. E., Sánchez Goñi, M. F., Couchoud, I., McDonald, J., Maas, R., Lohmann, G., Isola, I.: Evidence for obliquity forcing of Glacial termination II, Science, 325, 1527–1531, 2009.
Duplessy, J. C., Labeyrie, L., Juillet-Leclerc, A., Maitre, F., Duprat, J., and Sarnthein, M. : Surface salinity reconstruction of the North Atlantic Ocean during the last glacial maximum, Oceanol. Acta, 14, 311–324, 1991.
Franzese, A. M., Hemming, S. R., and Goldstein, S. L.: Use of strontium isotopes in detrital sediments to constrain the glacial position of the Agulhas Retroflection, Paleoceanography, 24, PA2217, doi:10.1029/2008PA001706, 2009.
Gordon, A. L.: The brawniest retroflection, Nature, 421, 904–905, 2003.
Greaves, M., Caillon, N., and Rebaubier, H., Bartoli, G., Bohaty, S., Cacho, I., Clarke, L., Cooper, M., Daunt, C., Delaney, M., deMenocal, P., Dutton, A., and Eggins, S., Elderfield, H., Garbe-Schoenberg, D., Goddard, E., Green, D., Groeneveld, J., Hastings, D., Hathorne, E., Kimoto, K., Klinkhammer, G., Labeyrie, L., Lea, D. W., Marchitto, T., Martınez-Botı, M. A., and Mortyn, P. G., Ni, T., Nuernberg, D., Paradis, G., Pena, L., Quinn, T., Rosenthal, Y., Russell, A., Sagawa, T., Sosdian, S., Stott, L., Tachikawa, K., Tappa, E., and Thunell, R., and Wilson, P. A.: Interlaboratory comparison study of calibration standards for foraminiferal Mg/Ca thermometry, Geochem. Geophy. Geosys., 9, Q08010, doi:10.1029/2008GC001974, 2008.
Huybers, P.: Glacial variability over the last two million years: an extended depth-derived age-model, continuous obliquity pacing, and the Pleistocene progression, Quat. Sci. Rev., 26, 37–55, 2007.
Huybers, P. and Denton, G.: Antarctic temperature at orbital timescales controlled by local summer duration, Nature Geosci., 1, 787–792, 2008.
Huybers, P. and Wunsch, C.: Obliquity pacing of the late Pleistocene glacial terminations, Nature, 434, 491–494, 2005.
Jouzel, J., Masson-Delmotte, V., Cattani, O., Dreyfus, G., Falourd, S., Hoffmann, G., Minster, B., Nouet, J., Barnola, J. M., Chappellaz, J., Fischer, H., Gallet, J. C., Johnsen, S., Leuenberger,

CPD
7, 2193–2215, 2011
High-latitude obliquity forcing drives the agulhas leakage
T. Caley et al.

M., Loulergue, L., Luethi, D., Oerter, H., Parrenin, F., Raisbeck, G., Raynaud, D., Schilt, S., Schwander, J., Selmo, E., Souchez, R., Spahni, R., Stauffer, B., Steffensen, J. P., Stenni, B., Stocker, T. F., Tison, J. L., Werner, M., and Wolff, E. W.: Orbital and Millennial Antarctic Climate Variability over the Past 800,000 Years, Science, 317, 793–796, 2007.

Khodri, M., Ramstein, G., Duplessy, J. C., Kageyama, M., Paillard, D., and Ganopolski, A.: Modelling the climate evolution from the last interglacial to the start of the last glaciation: The role of Arctic Ocean freshwater budget, Geophys. Res. Lett., 30, 1606, doi:10.1029/2003GL017108, 2003.

Kim, J. H., Meer, J. V. D., Schouten, S., Helmke, P., Willmot, V., Sangiorgi, F., Koç, N., Hopmans, E. C., and Sinninghe Damste, J. S.: New indices and calibrations derived from the distribution of crenarchaeal isoprenoid tetraether lipids: Implications for past sea surface temperature reconstructions, Geochim. Cosmochim. Acta, 74, 4639–4654, 2010.

Knorr, G. and Lohmann, G.: Southern Ocean origin for the resumption of Atlantic thermohaline circulation during deglaciation, Nature, 424, 532–536, 2003.

Laepple, T. and Lohmann, G.: Seasonal cycle as template for climate variability on astronomical timescales, Paleoceanography, 24, PA4201, doi:10.1029/2008PA001674, 2009.

Lisiecki, L. E.: Links between eccentricity forcing and the 100,000-year glacial cycle, Nature Geosci., 3, 349–352, 2010.

Lisiecki, L. E. and Raymo, M. E.: A Pliocene-Pleistocene stack of 57 globally distributed benthic δ^{18}O records, Paleoceanography, 20, PA1003, doi:10.1029/2004PA001071, 2005.

Lisiecki, L. E., Raymo, M. E., and Curry, W. B.: Atlantic overturning responses to Late Pleistocene climate forcings, Nature, 456, 85–88, doi:10.1038/nature07425, 2008.

Lohmann, G.: Atmospheric and oceanic freshwater transport during weak Atlantic overturning circulation, Tellus, Ser. A, 55, 438–449, 2003.

Lutjeharms, J. R. E.: The Agulhas Current, Springer, 2006.

Mann, M. E. and Lees, J. M.: Robust estimation of background noise and signal detection in climatic time series, Clim. Change, 33, 409–445, 1996.

Marsh, R., Hazeleger, W., Yool, A., and Rohling, E. J.: Stability of the thermohaline circulation under millennial CO2 forcing and two alternative controls on Atlantic salinity, Geophys. Res. Lett., 34, L03605, doi:10.1029/2006GL027815, 2007.

Martínez-Méndez, G., Zahn, R., Hall, I. R., Peeters, F. J. C., Pena, L. D., Cacho, I., and Negre, C.: Contrasting multiproxy reconstructions of surface ocean hydrography in the Agulhas Corridor and implications for the Agulhas Leakage during the last 345,000 years, Paleo-

ceanography, 25, PA4227, doi:10.1029/2009PA001879, 2010.
Müller, P., Kirst, G., Ruhland, G., von Storch, I., and Rosell-Melé, A.: Calibration of the alkenone paleotemperature index based on core-tops from the eastern South Atlantic and the global ocean (60′ N–60′ S), Geochim. Cosmochim. Acta, 62, 1757–1772, 1998.
Peeters, F., Acheson, R., Brummer, G. J. A., de Ruijter, W. P. M., Schneider, R. R., Ganssen, G. M., Ufkes, E., and Kroon, D.: Vigorous exchange between the Indian and Atlantic oceans at the end of the past five glacial periods, Nature, 430, 661–665, 2004.
Percival, D. B. and Walden, A. T.: Spectral analysis for physical applications: multitaper and conventional univariate techniques, Cambridge Uni. Press, Cambridge, 1993.
Prahl, F. G., Muehlhausen, L. A., and Zahnle, D. L.: Further evaluation of long-chain alkenones as indicators of paleoceanographic conditions, Geochim. Cosmochim. Acta, 52, 2303–2310, 1988.
Prahl, F. G. and Wakeham, S. G.: Calibration of unsaturation patterns in long-chain ketone compositions for paleotemperature assessment, Nature, 330, 367–369, 1987.
Press, W. H., Flannery, B. P., Teukolsky, S. A., and Vetterling, W. T.: Numerical recipes in Pascal: The art of scientific computing, Cambridge Uni. Press, Cambridge, 1990.
Rau, A. J., Rogers, J., Lutjeharms, J. R. E., Giraudeau, J., Lee-Thorp, J. A., Chen, M. T., and Waelbroeck, C.: A 450-kyr record of hydrological conditions on the western Agulhas Bank Slope, south of Africa, Mar. Geol., 180, 183–201, 2002.
Sijp, W. P. and England, M. H.: The effect of a northward shift in the southern hemisphere westerlies on the global ocean, Prog. Oceanog., 79, 1–19, 2008.
Suwa, M. and Bender, M. L.: Chronology of the Vostok ice core constrained by O^2/N^2 ratios of occluded air, and its implication for the Vostok climate records, Quat. Sci. Rev., 27, 1093–1106, 2008.
Van Sebille, E., Biastoch, A., van Leeuwen, P. J., and de Ruijter, W. P. M.: A weaker Agulhas Current leads to more Agulhas leakage, Geophys. Res. Lett., 36, L03601, doi:10.1029/2008GL036614, 2009.
Vimeux, F., Masson, V., Jouzel, J., Stievenard, M., and Petit, J. R.: Glacial-interglacial changes in ocean surface conditions in the Southern Hemisphere, Nature, 398, 410–413, 1999.
Von Storch, H. and Zwiers, F. W.: Statistical analysis in climate research. Cambridge Univ. Press., Cambridge, U. K., 735 pp., 1999.
Weijer, W., De Ruijter, W. P. M., Sterl, A., and Drijfhout, S. S.: Response of the Atlantic overturning circulation to South Atlantic sources of buoyancy, Global Planet. Change, 34, 293–311,

CPD
7, 2193–2215, 2011

Title Page
Abstract | Introduction
Conclusions | References
Tables | Figures
◀◀ | ▶▶
◀ | ▶
Back | Close
Full Screen / Esc
Printer-friendly Version
Interactive Discussion

2002.
Yoshimori, M., Weaver, A. J., Marshall, S. J., Clarke, G. K. C.: Glacial termination: Sensitivity to orbital and CO_2 forcing in a coupled climate system model, Clim. Dyn., 17, 571–588, 2001.
Zahn, R.: Beyond the CO_2 connection, Nature, 460, 335–336, 2009.

CPD
7, 2193–2215, 2011

High-latitude obliquity forcing drives the agulhas leakage

T. Caley et al.

Table 1. Phase and coherence between Agulhas surface proxies and $-1 \times \delta^{18}$Obenthic. The asterisks indicate that the coherence is not significant ($p = 0.05$). A negative phase indicates that the Agulhas surface records are leading δ^{18}Obenthic. In addition, phase and coherence between Antarctic temperature records and Agulhas SST stack record were calculated. A negative phase indicates that Agulhas SST stack is lagging Antarctic ice core records. Note that phase and coherence between the Vostok temperature record (Suwa and Bender, 2008) and Agulhas SST stack were calculated for an overlapping period (i.e. 0–411 kyr BP).

Proxy	Frequency	Phase	95 % confidence interval	Coherence
SST stack	100ky band	−14.4 kyr	±5.0 kyr	0.85
	41ky band	−2.2 kyr	±1.9 kyr	0.86
	21 ky band	−4.0kyr	±3.7 kyr	0.59
$\Delta\delta^{18}O_{SW}$	100 ky band	−12.8 kyr	±11.6 kyr	0.61
	41 ky band	−1.7 kyr	±6.1 kyr	0.54
	21 ky band	−1.5 kyr	±7.5 kyr	0.33*
EDC3	100ky band	−9.9 kyr	±4.9 kyr	0.85
(EDC3 chronology)	41 ky band	−1.1 kyr	±1.9 kyr	0.86
	21 ky band	−1.4 kyr	±5.4 kyr	0.37*
Vostok	100 ky band	−4.6 kyr	±4.8 kyr	0.83
(O_2/N_2 chronology)	41 ky band	1.9 kyr	±2.1 kyr	0.82
	21 ky band	0.7 kyr	±2.8 kyr	0.58

CPD
7, 2193–2215, 2011

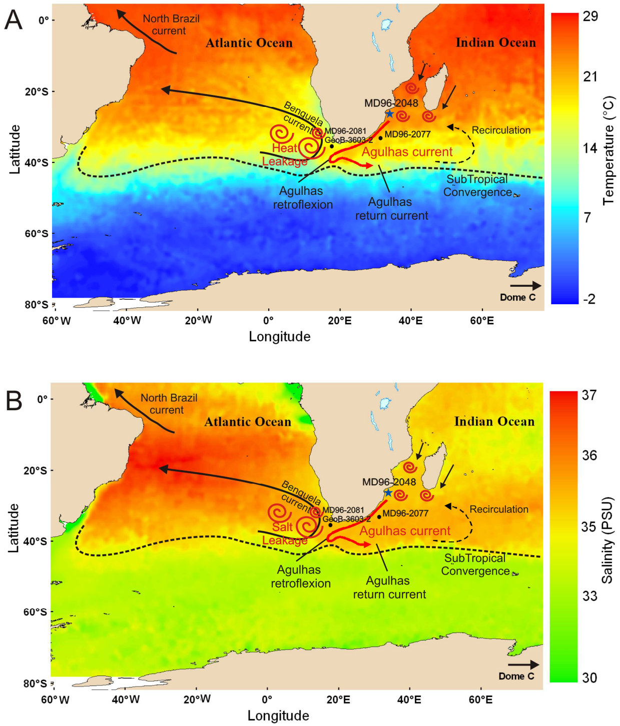

Fig. 1. Heat and salt transfer of the Agulhas surface current. **(A)** Sea surface temperature (SST) and **(B)** sea surface salinity (SSS) distribution pattern in the Agulhas system obtained from NODC_WOA94 data provided by the NOAA/OAR/ESRL PSD, Boulder, Colorado, USA, from their Web site (http://www.esrl.noaa.gov/psd/). The location of core MD96-2048 (blue star) and schematic views of the Agulhas current system (red arrows) are indicated. The position of the Subtropical Convergence (STC) is indicated by the black dashed line. Locations of the EPICA Dome C (EDC) site and sediment cores MD96-2081, GeoB-3603-2 and MD96-2077 are also indicated.

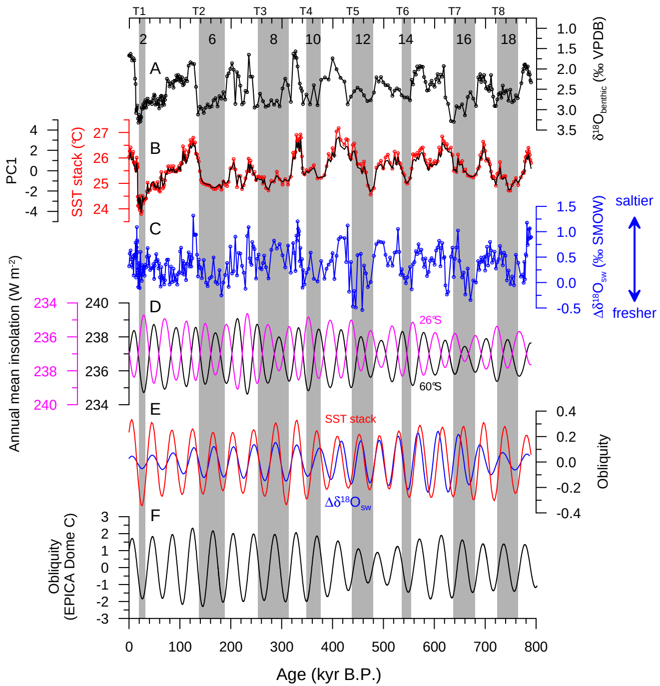

Fig. 2. Comparisons of MD96-2048 records with insolation and Antarctic climate record. **(A)** δ^{18}O of benthic foraminifer *P. wuellerstorfi*, **(B)** stacked record of Mg/Ca, $U_{37}^{K'}$, and TEX_{86}^{H} SSTs (red line) and first order of Principal Component (PC1, black line) derived from EOF analysis, **(C)** reconstructed $\Delta\delta^{18}O_{sw}$ (a proxy of regional sea surface salinity), **(D)** obliquity components (frequency 1/41000; bandwidth: 5×10^{-6}) of SST stack (red) and $\Delta\delta^{18}O_{sw}$ (blue), **(E)** annual mean insolation at 60° S or 60° N (black) and 26° S (purple) calculated according to Berger and Loutre, (1991), and **(F)** obliquity components (frequency 1/41000; bandwidth: 5×10^{-6}) of atmospheric temperatures of EPICA Dome Concordia (EDC), Antarctica (Jouzel et al., 2007). *T* indicates terminations and numbers indicate marine isotopic stages (MIS).

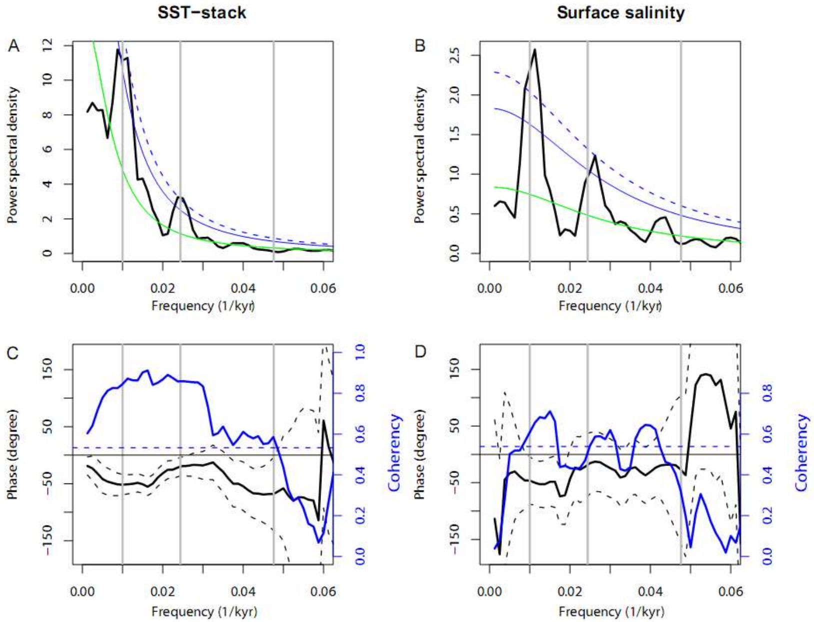

Fig. 3. Frequency spectra for Agulhas proxies (SST and SSS) and their coherence and phase relationship relative to global ice volume (δ^{18}**O**$_{\text{benthic}}$). **(A)** power spectral density of SST (black). A red noise background spectrum (green) and 95 % (blue continuous) and 99 % (blue dashed) confidence levels, relative to the red-noise background are given. **(B)** as **(A)** but for SSS. **(C)** coherence (blue) and phase (black) between the SST proxy and $-1 \times \delta^{18}O_{\text{benthic}}$. The approximate 95 % con?dence level for the coherence (blue dashed line) and the 95 % con?dence interval for phase (black dashed line) are given. **(D)** as **(C)** but for the SSS and $-1 \times \delta^{18}O_{\text{benthic}}$ relationship. Negative phase indicates that the Agulhas records are leading $-1 \times \delta^{18}O_{\text{benthic}}$. The orbital frequencies 1/100 kyr, 1/41 kyr and 1/21 kyr are marked with vertical grey lines.

CPD
7, 2193–2215, 2011

High-latitude obliquity forcing drives the agulhas leakage

T. Caley et al.

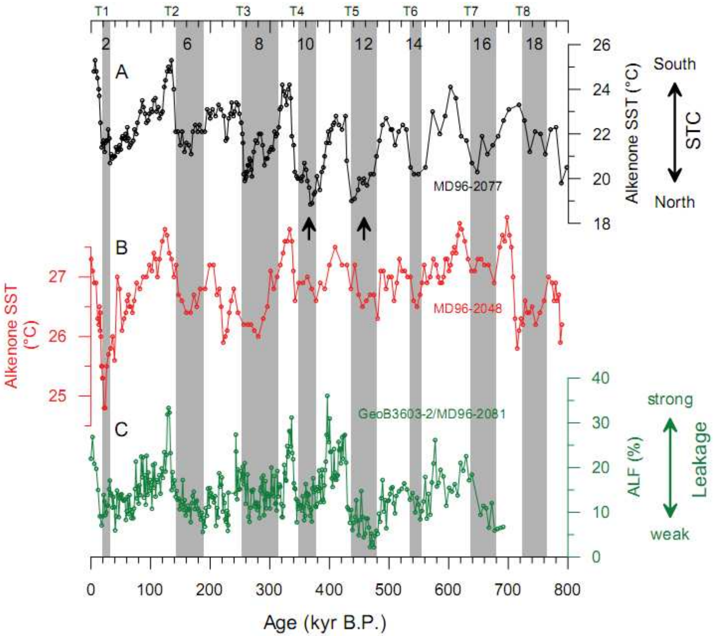

Fig. 4. Relationship between the subtropical convergence (STC) migration and the AC strength and transfer. **(A)** $U^{K'}_{37}$ SST record of MD96-2077, which was used as a proxy of STC migration (Bard and Rickaby, 2009), **(B)** $U^{K'}_{37}$ SST record at site MD96-2048. Warmer glacial SSTs were observed in our record when the STC reached its northern most position (black arrows), and **(C)** Agulhas leakage fauna (ALF) record compiled from GeoB3603-2 and MD96-2081, a foraminiferal proxy of the Agulhas leakage (Peeters et al., 2004). Note that a new age model for GeoB3603-2 and MD96-2081 was build based on the correlation between the δ^{18}O of the benthic foraminifer and the LR04 stack (Lisiecki and Raymo, 2005) to allow comparison with our dataset. AC denotes the Agulhas Current.